

Optimized Pre-Processing Strategy for the Correction of Gradient Field Inhomogeneities in 3D-PC-MRI

D. Giese¹, J. Bock¹, A. Stalder¹, R. Lorenz¹, and M. Markl¹

¹Dept. of Diagnostic Radiology, Medical Physics, University Hospital Freiburg, Freiburg, Germany

Introduction: Flow sensitive phase contrast (PC) MRI has been widely applied for the assessment of cardiovascular function [1]. Recently, time-resolved 3D PC-MRI with three-directional velocity encoding (flow sensitive 4D-MRI) has gained increased importance. A number of studies have shown that flow sensitive 4D-MRI can be used for the detailed visualization and quantification of 3D blood flow within entire vascular structures such as the thoracic aorta [2, 3], intra-cranial arteries [4], the heart [5], or peripheral vessels [6]. However, compared to traditional 2D-CINE-PC techniques, data acquisition with such 4D methods can extend over large 3D volumes and may suffer from increased velocity encoding errors due to gradient system non-linearities. Since such errors increase with increasing distance from the magnet's isocenter, artifacts in phase contrast measurements due to gradient imperfections can have considerable effects for large vascular structures. The additional effect of spatial image warping has been efficiently investigated leading to a systematic correction option on today's scanners. Impact of gradient inhomogeneities on phase images have previously also been analyzed and correction algorithms were proposed [7]. However, to date, none of the commercially available MR systems include corrections for gradient field based velocity errors. The aim of this study was to provide a comprehensive correction and data pre-processing strategy for flow sensitive 4D-MRI. Gradient field compensation was integrated into an interactive tool [8] for data pre-processing including noise masking, eddy current and velocity aliasing correction. Furthermore, the correction process was applied to two phantom studies to illustrate and quantify the effect of gradient field distortions for large 3D volumes and common in-vivo routine parameters.

Materials and Methods: Two phantoms were used: #1 a gel cylinder rotated by a pressured air supply, #2 a realistic model of the thoracic aorta embedded into a flow circuit driven by a pulsating flow pump. Phantom #2 was used to provide a realistic model for simulating in-vivo pulsatile 3D flow within the thoracic aorta and could thus be used to evaluate gradient field errors in a controlled setting simulating the in-vivo situation. All measurements were performed on a 3T system (Trio, Siemens, Germany) using a three dimensional velocity encoded ECG gated CINE PC sequence. Phantom #1 was placed off-center (20.5 cm distance to the isocenter) to evaluate the correction algorithms (2D Coronal slice, FOV: 500x500mm, resolution: 1.95x1.95x8 mm, $v_{enc}=100\text{cm/s}$, temporal resolution: 18ms). For Phantom #2 simulating in-vivo conditions, routine imaging parameters were used (3D Slab, FOV: 320x220mm, resolution: 2.29x1.25x2 mm, $v_{enc}=150\text{cm/s}$, temporal resolution: 41.6ms). All acquisitions were geometrically unwarped before correction. Images were then processed using the tool, including an anti-aliasing filter, a noise filter, followed by the gradient inhomogeneity correction based on the general reconstruction method [7]. The corrected images were further analyzed using in-house analysis tools based on Matlab (MathWorks, USA).

Results: As expected, effects of gradient non-uniformities were not negligible. Fig.1 shows velocity images of a coronal slice through the rotational phantom before and after pre-processing. Although geometrical unwarping of the uncorrected images was performed, the gradient inhomogeneities cause distortions in the velocity measurements. Application of the proposed processing chain successfully removed background noise and corrected the gradient field distortions. Comparison with velocities derived from the known phantom rotation frequency demonstrated excellent agreement of corrected and expected velocities (Fig.1 and 2). Table 1 quantifies the correction and shows a reduction of the relative errors compared to the simulated theoretical images. Mean error reduction of up to 95% of uncorrected velocity errors demonstrates the high correction impact. The distribution and extent of gradient field induced errors for the aorta phantom are displayed in Fig.3 (a,b,c). The images show a maximum intensity projection (MIP) of the relative errors for each encoding direction for a time frame with maximum flow. Results indicate a maximum error and thus reveal a correction impact of up to 14% of the used v_{enc} value. As expected, velocity errors substantially increase near the edges of the 3D volume. Moreover, gradient distortions affect the velocity direction (by distorting each velocity encoding direction independently). This is shown in Fig.3 (d,e,f) which depicts angular data, representing the error MIP's of each spherical coordinate (radial distance r , azimuth θ and zenith angle Φ) of the velocity vector. Finally, using an in-house flow quantification tool [9], the impact of gradient field correction on flow quantification was verified. The flow volume through a single vessel at three different locations (Fig.4) was calculated, revealing a clear improvement in blood flow quantification and thereby preserving average flow through a single vessel.

Discussion: The presented tool allows the correction of three dimensional phase contrast data including errors due to gradient nonuniformities. The results have shown that for common in-vivo routine parameters, data may include velocity magnitude errors of up to 14% and angular errors of up to 50 degrees arising from gradient inhomogeneities. Current results show that quantitative data extracted from PC measurements such as blood flow volume can include errors leading to inconsistencies along individual vessels. Correcting data prior to analysis using the presented tool may therefore have the potential to provide a standardized way to improve quantification results. Future work will include in-vivo analysis and comparison of corrected and non-corrected flow data as well as analysis of the impact of gradient field non-linearities on 3D flow visualization using 3D stream-lines or particle-traces. Moreover, additional sources of errors (Maxwell terms, acceleration effects) need to be included into the data pre-processing chain.

Acknowledgements: Grant support by the Deutsche Forschungsgemeinschaft (DFG), Grant # MA 2383/4-1, and the Bundesministerium für Bildung und Forschung (BMBF), Grant # 01EV0706.

References: [1] Pelc NJ et al, Magn Reson Q 1991;7(4):229-254 [2] Bogren HG et al, J Magn Reson Imaging 1999;10(5):861-869 [3] Markl M et al, J Magn Reson Imaging 2007;25(4):824-831 [4] Wetzel S et al, AJNR Am J Neuroradiol 2007;28(3):433-438 [5] Kilner PJ et al, Nature 2000;404(6779):759-761 [6] Frydrychowicz A et al, J Magn Reson Imaging 2007;25(5):1085-1092 [7] Markl M et al, Magn Reson Med 2003;50:791-801 [8] Bock J et al Proc ISMRM Berlin, Germany 2007;3139 [9] Stalder et al ISMRM Berlin, Germany 2007;3139

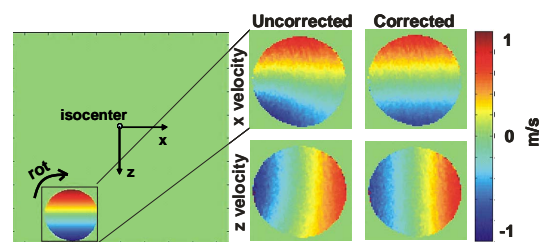


Fig.1: Uncorrected and Corrected x and z velocity images

	uncorrected			corrected		
	max	min	mean	max	min	mean
Velocity x	56.45	-44.45	-0.0615	40.02	-37.22	-0.0046
Velocity y	37.7	-13.77	0.64	38.36	-53.7	0.0122
Velocity z	175.02	-24.41	-0.26	163.03	-109.55	0.0123
Angle	623.82	-625.77	-0.62	611.41	-62.89	-0.11

Table1: Relative errors in % to the expected values

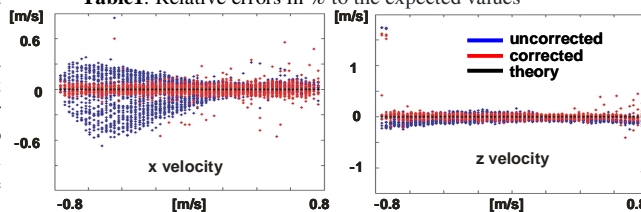


Fig.2: Velocity errors plotted over theoretical velocities. The uncorrected errors show a larger dispersion than the corrected.

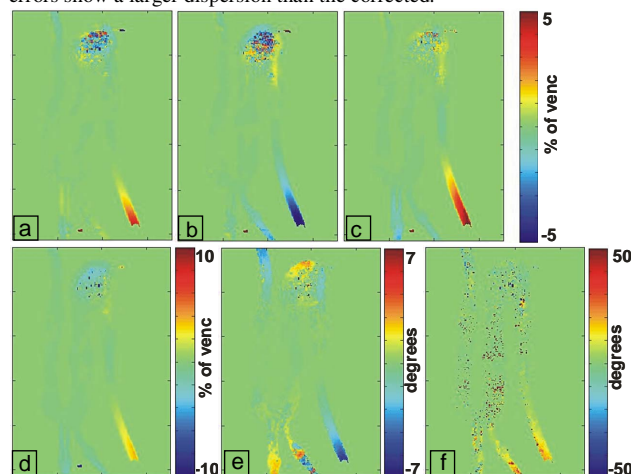


Fig.3: Error MIP's for x,z,y velocities (a,b,c) and their spherical coordinates r, θ, Φ (d,e,f)

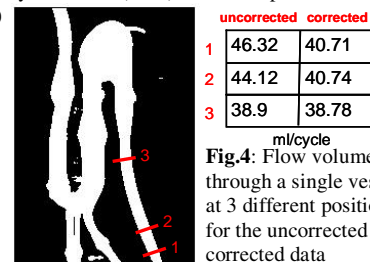


Fig.4: Flow volume through a single vessel at 3 different positions for the uncorrected and corrected data